Contribution from the Department of Chemistry, Franklin & Marshall College, Lancaster, Pennsylvania 17604, and Department of Chemistry and Materials Research Center, Northwestern University, Evanston, Illinois 60208

# Polarized Specular Reflectance Spectra of the Partially Oxidized Phthalocyanines Cu(pc)I and $H_2$(pc)I Compared with Those of Co(pc)I and Ni(pc)I: Metal-Based Charge-Transfer Transitions in One-Dimensional Conductors

Dean E. Rende,[1a] Michael D. Heagy,[1a] William B. Heuer,[1a,b] Kwangkyoung Liou,[1c] Julia A. Thompson,[1c] Brian M. Hoffman,*[,1c] and Ronald L. Musselman*[,1a]

*Received June 21, 1991*

Polarized single-crystal ultraviolet and visible specular reflectance spectra and Kramers-Kronig-transformed absorbance spectra of Cu(pc)I and $H_2$(pc)I allow clarification of metal-based charge-transfer transitions, especially when compared with earlier results on Ni(pc)I and Co(pc)I and recent calculations. Earlier out of plane assignments have been confirmed, and some modified assignments are proposed for in-plane transitions, including the well-known Soret transition.

Phthalocyanines (pc's) have long been of interest because of their intense electronic transitions in the visible region,[2-5] which render them useful as textile dyes, and their similarity to porphyrins, which has led to their use as models for electronic structure in biological systems.[3,4] Several reviews of pc spectra and electronic structure studies are available.[2-4,6-8] In the solid state the large planar molecules stack closely enough for interaction between planes,[9-11] enabling them to serve as thin-film conductors and electrode media.[12-14] When partially oxidized, they arrange into straight stacks of macrocycles (with the interstitial channels containing the oxidant), becoming one-dimensional conductors or semiconductors.[15-20] Conduction in iodinated metallophthalocyanines (M(pc)I's) appears to occur through different routes depending upon the central metal: when M = Ni, Cu, or $H_2$, conductivity is associated with a ligand-based band formed by the overlap of the $\pi$ orbitals,[17,18,20] and when M = Co, the electronic conductivity is along the metal spine through a band formed by the $d_{z^2}$ orbitals.[19] We recently reported on the UV-visible reflectance spectra of Co(pc)I and Ni(pc)I in which two new charge-transfer transitions were observed: $a_{1g}(d_{z^2}) \rightarrow a_{2u}(p_z,\pi^*)$ and $b_{2u}(\pi) \rightarrow b_{1g}(d_{x^2-y^2})$.[21] The $a_{1g} \rightarrow a_{2u}$ transition had not been observed in earlier IR-vis specular reflectance[17,19] but was suggested by our Kramers-Kronig transformation of our UV-vis data into absorption values because of slight structure appearing on a band previously attributed to the $I_3^-$ ion in the crystal.[17,19] Deconvolution of this band using structurally similar $I_3^-$ salts as a guide revealed an $a_{1g} \rightarrow a_{2u}$ peak to the red of the $I_3^-$ transition in both the Ni and Co cases. These metal-to-ligand and ligand-to-metal charge-transfer bands are of interest because they give information about energies of predominantly metal orbitals relative to predominantly ligand orbitals. These orbital energies ultimately determine the site of partial oxidation and hence the conduction mechanisms in these compounds.

Our interest in M(pc)I's is an outgrowth of an ongoing program to understand the spectroscopy of one-dimensional molecular crystals containing closely interacting planar transition-metal complexes.[22-26] Simpler systems such as tetracyanoplatinates[23,27] and bis(dimethylglyoximato)nickel[28] show strong red shifts and dramatic intensity increases in transitions involving orbitals related to one-dimensional conductivity upon crystallization from solution and upon formation of more closely stacked salts or exertion of high pressures.[29,30] Since neither band formation[31] nor exciton formation[32] alone appears to be sufficient to describe these red shifts, we are studying a wide range of planar complexes having close interactions in order to determine the origin of the shifts. Identification of metal-related transitions in M(pc)I's is thus an important part of this larger study.

The set of metals Co, Ni, and Cu provides a trend in energies of metal-based orbitals that assists in identifying metal-related transitions within complexes of this type. In this work, we wished to add Cu(pc)I to our earlier work on Co(pc)I and Ni(pc)I.[21] However, the most prominent metal-related transitions in Cu(pc)I fall at the same energies as $I_3^-$ transitions extracted earlier via Gaussian deconvolution (vide infra). In order to permit unambiguous identification of the $I_3^-$ transitions in these partially oxidized phthalocyanines, we have therefore also made a parallel study of the metal-free $H_2$(pc)I.

Both $H_2$(pc)I and Cu(pc)I are isomorphous with Ni(pc)I and Co(pc)I and exhibit metal-like conductivity mediated by ligand-based $\pi$ bands as demonstrated by EPR, magnetic susceptibility, thermoelectric power, and temperature-dependent conductivity

* To whom correspondence should be addressed.

(1) (a) Franklin & Marshall College. (b) Camille and Henry Dreyfus Teaching/Research Fellow. Current address: Chemistry Department, United States Naval Academy, Annapolis, MD 21402. (c) Northwestern University.
(2) Lever, A. B. P. *Adv. Inorg. Radiochem.* **1965**, *7*, 28.
(3) Sayer, P.; Gouterman, M.; Connell, C. R. *Acc. Chem. Res.* **1982**, *15*, 73.
(4) Hoffman, B. M.; Ibers, J. A. *Acc. Chem. Res.* **1983**, *16*, 15.
(5) Chen, I. *J. Mol. Spectrosc.* **1967**, *23*, 131.
(6) Gouterman, M. *J. Mol. Spectrosc.* **1961**, *6*, 138.
(7) Gouterman, M. In *The Porphyrins*; Dolphin, D., Ed.; Academic Press: New York, 1978; pp 1-166.
(8) Nyokong, T.; Zbigniew, G.; Stillman, M. *Inorg. Chem.* **1987**, *26*, 1087.
(9) Robertson, J. M.; Woodward, I. *J. Chem. Soc.* **1938**, 219.
(10) Williams, G. A.; Figgis, B. N.; Mason, R.; Mason, S. A.; Fielding, P. E. *J. Chem. Soc., Dalton Trans.* **1980**, 1688.
(11) Mason, R.; Williams, G. A.; Fielding, P. E. *J. Chem. Soc., Dalton Trans.* **1979**, 676.
(12) Lever, A. B. P.; Pickens, S. R.; Minor, P. C.; Licoccia, S.; Ramaswamy, B. S.; Magnell, K. *J. Am. Chem. Soc.* **1981**, *103*, 6800.
(13) Wiemhofer, H. D.; Schmeisser, D.; Gopel, W. *Solid State Ionics* **1990**, *40-1*, 421.
(14) Gould, R. D.; Hassan, A. K. *Thin Solid Films* **1990**, *193*, 895.
(15) Palmer, S. M.; Stanton, J. L.; Hoffman, B. M.; Ibers, J. A. *Inorg. Chem.* **1986**, *25*, 2296.
(16) Schramm, C. J.; Scaringe, R. P.; Stojakovic, D. R.; Hoffman, B. M.; Ibers, J. A.; Marks, T. J. *J. Am. Chem. Soc.* **1980**, *102*, 6702.
(17) Martinsen, J.; Palmer, S. M.; Tanaka, J.; Greene, R. C.; Hoffman, B. M. *Phys. Rev. B* **1984**, *30*, 6269.
(18) Inabe, T.; Marks, T. J.; Burton, R. L.; Lyding, J. W.; McCarthy, W. J.; Kannewurf, C. R. *Solid State Commun.* **1985**, *54*, 501.
(19) Martinsen, J.; Stanton, J. L.; Greene, R. L.; Tanaka, J.; Hoffman, B. M.; Ibers, J. A. *J. Am. Chem. Soc.* **1985**, *107*, 6915.
(20) Ogawa, M. Y.; Martinsen, J.; Palmer, S. M.; Stanton, J. L.; Tanaka, J.; Greene, R. L.; Hoffman, B. M.; Ibers, J. A. *J. Am. Chem. Soc.* **1987**, *109*, 1115.
(21) Heagy, M. D.; Rende, D. E.; Shaffer, G. W.; Wolfe, B. M.; Liou, K.; Hoffman, B. M.; Musselman, R. L. *Inorg. Chem.* **1989**, *28*, 283.
(22) Musselman, R. L.; Williams, J. W. *J. Chem. Soc., Chem. Commun.* **1977**, 186.
(23) Anex, B. G.; Musselman, R. L. *J. Phys. Chem.* **1980**, *84*, 883.
(24) Musselman, R. L.; Stecher, L. C.; Watkins, S. F. *Inorg. Chem.* **1980**, *19*, 3400.
(25) Musselman, R. L.; Cornelius, J. B.; Trapp, R. M. *Inorg. Chem.* **1981**, *20*, 1931.
(26) Musselman, R. L.; Anex, B. G. *J. Phys. Chem.* **1987**, *91*, 4460.
(27) Moreau-Colin, M. L. *Struct. Bonding* **1972**, *10*, 167.
(28) Anex, B. G.; Krist, F. K. *J. Am. Chem. Soc.* **1967**, *89*, 6114.
(29) Gliemann, G.; Yersin, H. *Struct. Bonding* **1985**, *62*, 87.
(30) Lechner, A.; Gliemann, G. *J. Am. Chem. Soc.* **1989**, *111*, 7469.
(31) Whangbo, M. H.; Hoffman, R. *J. Am. Chem. Soc.* **1978**, *100*, 6093.
(32) Day, P. *J. Am. Chem. Soc.* **1975**, *97*, 1588.

0020-1669/92/1331-0352$03.00/0 © 1992 American Chemical Society

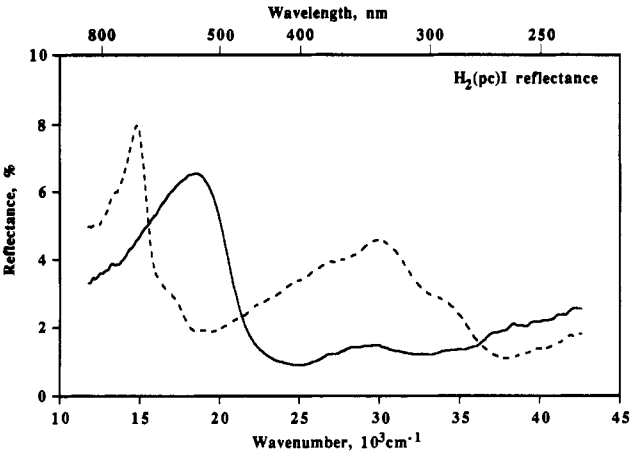


**Figure 1.** Polarized specular reflectance of $H_2$(pc)I: (—) electric vector parallel to needle (out-of-plane); (- - -) electric vector perpendicular to needle (in-plane).

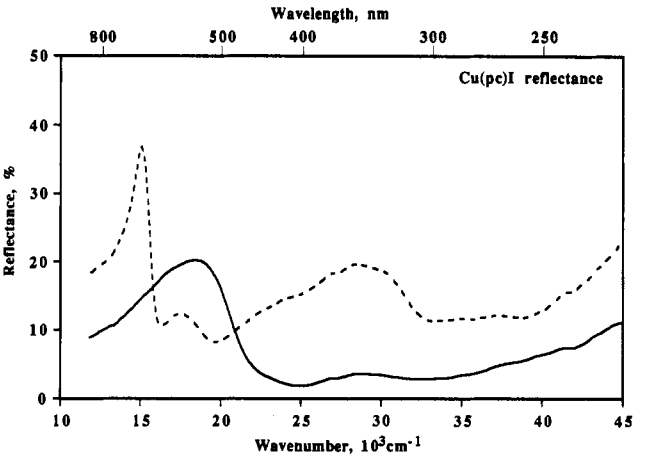


**Figure 2.** Polarized specular reflectance of Cu(pc)I: (—) electric vector parallel to needle (out-of-plane); (- - -) electric vector perpendicular to needle (in-plane).

studies.[18,20,33] We report here on the polarized electronic reflectance and derived absorbance spectra of $H_2$(pc)I and of Cu(pc)I and assign transitions on the basis of the behavior (or absence) of metal-related transitions in the $H_2$-, Co-, Ni-, and Cu(pc)I series and upon more recent calculations,[34-37] including the established "four-orbital model" for porphyrin systems,[6,7,38] and initial results from self-consistent-field density of states (DOS) calculations on several metalloporphyrins including Co-, Ni-, and Cu(pc).[37] (Recent DV-X$\alpha$ calculations[39] on several M(pc)'s including Co(pc) will not be used since the calculations were optimized for ground-state properties and thus differ somewhat from the DV-X$\alpha$-DOS calculations[37] emphasizing transition energies.) The calculations have indicated a need for reassignment of two of the in-plane transitions in Co and Ni(pc)I, and the experimental results on Cu- and $H_2$(pc)I have allowed assignment of an additional out-of-plane transition in Co- and Ni(pc)I.

## Experimental Section

Single crystals of $H_2$(pc)I and Cu(pc)I were prepared as described elsewhere,[18,33] and specimens ~0.030 × 0.030 × 1 mm were selected for study.

Polarized specular reflectance spectra were obtained on an instrument based on a concept by Anex.[40] The instrument is essentially a grating microspectrophotometer consisting of tungsten-halogen and xenon arc light sources, an Instruments SA HR320 0.32-m computer-controllable grating monochromator, a Glan-Thompson polarizer, a double-beam reflecting microscope, and a photomultiplier detector. Signal detection is through two Princeton Applied Research 186A lock-in amplifiers, and instrument control resides on an Apple IIe computer. Data for each spectral point are collected until the sample mean has a 99% probability of being within 1% of the population mean. The data are then uploaded to a Hewlett-Packard 3000 computer for processing. Reflectance is measured relative to an NIST standard second-surface aluminum mirror, and Kramers-Kronig transformation of the average of at least three reflectance spectra is performed to obtain standard absorbance values.

Spectra were obtained from natural elongated faces of $H_2$(pc)I and Cu(pc)I with an illumination spot size of ~25 $\mu$m having the electric vector of the plane-polarized light aligned parallel to the needle (*c*) axis for "out-of-plane" spectra and perpendicular to the needle axis for "in-plane" spectra. The straight stacking of the macrocycles[18,20] provided the same molecular projections on all elongated faces. While $H_2$(pc) formally has $D_{2h}$ symmetry and thus should provide two distinct in-plane spectra,[41] in $H_2$(pc)I, the macrocycles are alternately rotated 40°,[18] which prevents the observation of in plane differences. Reflectances from beyond experimentally accessible regions necessary for Kramers-Kronig analyses were estimated for the far ultraviolet in order to give zero absorbance in the resultant transformation where vapor state absorbance is zero. Reflections were used with maxima of 10% and 30% at ~51 × $10^3$ $cm^{-1}$ for $H_2$(pc)I and Cu(pc)I, respectively. Low-energy values were based upon IR reflectance from $H_2$(pc)I[18] for the $H_2$ and similar systems[17,19] for the Cu complex. Deconvolution was carried out with an

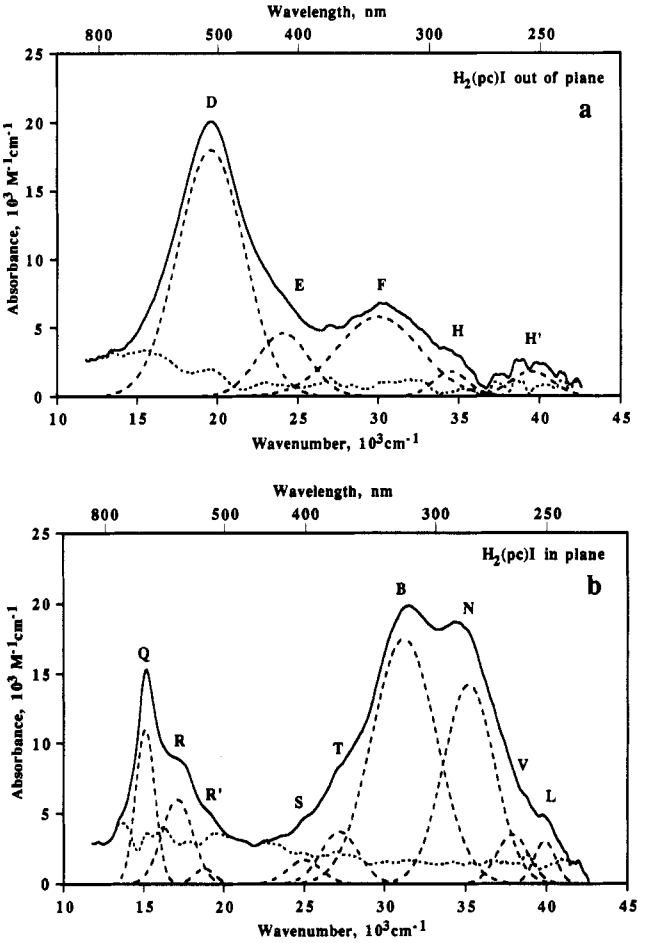


**Figure 3.** (a) Out-of-plane and (b) in-plane absorbance from specular reflectance of $H_2$(pc)I: (—) experimental, (- - -) Gaussian deconvolution; (···) residual baseline.

(33) Thompson, J. A.; Murata, K.; McGhee, E. M.; Stanton, J. L.; Rende, D. E.; Broderick, W. E.; Musselman, R. L.; Hoffman, B. M.; Ibers, J. A. To be submitted for publication in *Inorg. Chem.*
(34) Kutzler, F. W.; Ellis, D. E. *J. Chem. Phys.* **1986**, *84*, 1033.
(35) Henriksson, A.; Sundbom, M. *Theoret. Chim. Acta* **1972**, *27*, 213.
(36) Henriksson, A.; Roos, B.; Sundbom, M. *Theoret. Chim. Acta* **1972**, *27*, 303.
(37) Liang, X.; Flores, S.; Ellis, D. E.; Hoffman, B. M.; Musselman, R. L. *J. Chem. Phys.* **1991**, *95*, 403.
(38) Wang, M.-Y. R.; Hoffman, B. M. *J. Am. Chem. Soc.* **1984**, *106*, 4235.
(39) Reynolds, P. A.; Figgis, B. N. *Inorg. Chem.* **1991**, *30*, 2294-2300.
(40) Anex, B. G. *Mol. Cryst.* **1966**, *1*, 1.
(41) Anex, B. G. *J. Am. Chem. Soc.* **1964**, *86*, 5026.

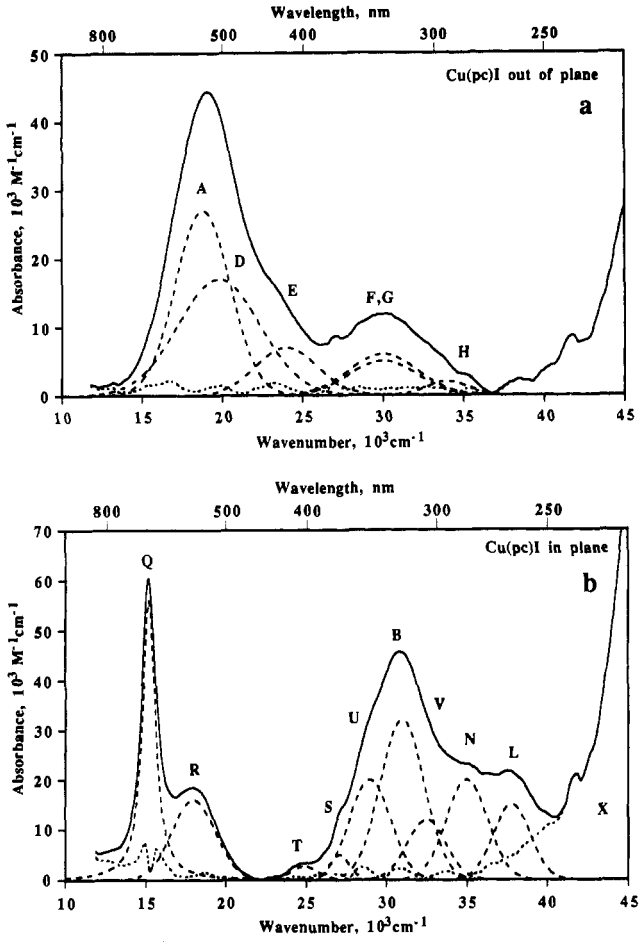


**Figure 4.** (a) Out-of-plane and (b) in-plane absorbance from specular reflectance of Cu(pc)I: (—) experimental, (---) deconvolution, (···) residual baseline.

interactive Gaussian and Lorentzian analysis program on the HP3000 computer.

## Results and Discussion

The polarized specular reflectance spectra for $H_2$(pc)I and Cu(pc)I are shown in Figures 1 and 2, respectively, and the corresponding Kramers–Kronig transformations along with deconvolutions are shown in Figures 3 and 4, respectively. The $H_2$(pc)I reflectance spectra agree qualitatively with those obtained earlier and reported as reflectance only.[18] As noted above, the $H_2$(pc)I spectra provide a convenient "background" for identification of metal-based transitions ($d_{z^2} \rightarrow p_z$ and $\pi \rightarrow d_{x^2-y^2}$) in the M(pc)I (M = Co, Ni, Cu) series, since these transitions must be *absent* in $H_2$(pc)I.

**Out-of-Plane Transitions.** Figure 3a shows prominent peaks at 19.6 × $10^3$ $cm^{-1}$ (D)[42] and 30.0 $kcm^{-1}$ (F), consistent with peaks identified earlier[21,43] as $I_3^-$ transitions $^1\Sigma_g \rightarrow {}^1\Sigma_u^*$ ($\sigma_g \rightarrow \sigma_u^*$) and a spin–orbit coupling component, respectively (The peak identification scheme follows that of Platt[42] only for the Q, B, N, L, and C bands, which have been used by others for phthalocyanines;[8,21] the remainder of our peak labels are arbitrary). The excellent agreement in energy, intensity, and band shape between these two peaks and the equivalent deconvoluted peaks in Co(pc)I and Ni(pc)I confirms our Gaussian deconvolution of the ~(15–20) × $10^3$ $cm^{-1}$ peaks in spectra of the latter complexes.[21] Theoretical confirmation of an $I_3^-$ transition near 20 × $10^3$ $cm^{-1}$ comes from recent calculations predicting a strong needle-axis-polarized peak at 17.2 × $10^3$ $cm^{-1}$ due to $I_3^-$.[37]

Peak E at 24.1 × $10^3$ $cm^{-1}$ in Figure 3a could be due to either the pc macrocycle or $I_3^-$, since it shows no change from $H_2$(pc)I to Cu(pc)I and also appeared at 25 × $10^3$ $cm^{-1}$ in Co(pc)I.[21] A new deconvolution of the Ni(pc)I out of plane spectrum based upon the more accurate $^1\Sigma_g \rightarrow {}^1\Sigma_u^*$ transition parameters from $H_2$(pc)I also shows a peak at 24.5 × $10^3$ $cm^{-1}$ (Figure 7). Spectra of Co(tbp)I (tbp = tetrabenzoporphyrin)[44] show a similar peak at 25.0 × $10^3$ $cm^{-1}$. Tbp ligand orbital levels show experimental evidence[45] of being lower in energy than those in M(pc)I's although calculations have shown them to be both higher[37] and lower[34] in the Ni case. It is thus difficult to predict if one would expect a difference for tbp ligand transitions. Careful examination of spectra of solids having $I_3^-$ groups oriented linearly as in the M(pc)I's such as in $tbaI_3$, $(bza)_2HI_3$ and caf·$H_2O$·$HI_3$ (tba = tetra-*n*-butylammonium; bza = benzamide; caf = caffeine) shows a shoulder at ~25 × $10^3$ $cm^{-1}$,[43] while solutions containing $I_3^-$ show no such transition.[45] The peak also fails to appear in out of plane polarized spectra of $[Ni(tmp)]_2ReO_4$ (where tmp = tetramethylporphyrin), which exhibits similar face-to-face stacking of macrocycles but does not contain $I_3^-$.[45] Since tmp is similar to both pc and tbp, one would not expect the peak to disappear due to this ligand change. It may be reasonably suggested that the lack of $I_3^-$ caused the disappearance. We therefore propose that peak E is due to $I_3^-$, but only in the solid state, probably from collective interactions between the $I_3^-$ ions arranged colinearly. Peaks H and H' at 34.5 × $10^3$ and 39.2 × $10^3$ $cm^{-1}$ are weak peaks that also appear weakly in Cu-, Ni-, and Co(pc)I spectra. These are not predicted in calculations that we are aware of, so they remain unassigned at this time.

The out-of-plane Cu(pc)I absorbance spectrum, transformed from reflectance, is shown in Figure 4a. The intensity around 20 × $10^3$ $cm^{-1}$ may be considered to arise from peak A at 18.8 × $10^3$ $cm^{-1}$ and peak D at 19.8 × $10^3$ $cm^{-1}$. The position and intensity of D agree with the analogous peak in $H_2$(pc)I, and thus this peak may be assigned as an $I_3^- {}^1\Sigma_g \rightarrow {}^1\Sigma_u^*$ transition. Peak A corresponds to the $12a_{1g}(d_{z^2}) \rightarrow 6a_{2u}(\pi^*,p_z)$ transitions previously assigned in Co(pc)I and Ni(pc)I[21] and may be assigned as such in this case also. Table I shows that the energy of this transition increases upon substituting Cu for Co, in qualitative agreement with the expected energies of the $d_{z^2}$ orbitals in these metals and in agreement with recent calculations.[37] Peak E is assigned, as in $H_2$(pc)I, to $I_3^-$ in the solid state. The peak at 30 × $10^3$ $cm^{-1}$ appears larger than would be expected if it were due only to $I_3^-$ as other 30 × $10^3$ $cm^{-1}$ peaks have been.[21] The intensity ($\epsilon_{max}\Delta\bar{\nu}_{1/2}$) of the experimental peak is 85 × $10^3$ $M^{-1}$ $cm^{-2}$, while the expected intensity based upon the intensity of peak D and the relative intensities of peaks D and F in $H_2$(pc)I (Figure 3a) is 33 × $10^3$ $M^{-1}$ $cm^{-2}$. We thus propose that a second peak lies at 30 × $10^3$ $cm^{-1}$ in addition to the $I_3^-$ spin–orbit component. To guide our assignment of this additional transition, we will consider the $b_{2u}(\pi) \rightarrow b_{1g}(d_{x^2-y^2})$ transitions in Co(pc)I and Ni(pc)I.[21] These transitions appear at 40.5 × $10^3$ and 35.3 × $10^3$ $cm^{-1}$, respectively, and the energy difference agrees with the expected energy levels of the $d_{x^2-y^2}$ orbitals.[46] Continuation of this trend to Cu(pc)I would place a transition near 30 × $10^3$ $cm^{-1}$. We therefore have placed two transitions, F and G, under the 30 × $10^3$ $cm^{-1}$ peak and assign them as an $I_3^-$ spin–orbit coupling component and $3b_{2u}(\pi) \rightarrow 11b_{1g}(d_{x^2-y^2})$, respectively. Our orbital numbering follows that presented by Ellis et al.[37] for in-plane transitions involving these orbitals. It should be noted that no significant *z*-polarized transitions were calculated using the density of states method. This is possibly due to the use of monomers for the calculations. It has been shown experimentally that some metal-related transitions increase dramatically in intensity upon close approaches to neighbors in the solid state.[29,30]

Overviews of the out-of-plane transitions are presented in Figure 5a,b. The differences in the peak maxima of the ~20 × $10^3$ $cm^{-1}$ peaks are clearly visible in Figure 5a. The MLCT transition $12a_{1g}(d_{z^2}) \rightarrow 6a_{2u}(\pi^*,p_z)$ and the LMCT transition $3b_{2u}(\pi) \rightarrow$

(42) Platt, J. R. *J. Opt. Soc. Am.* **1953**, *43*, 252.
(43) Mizuno, M.; Tanaka, J.; Harada, I. *J. Phys. Chem.* **1981**, *85*, 1789.
(44) Liou, K.; Newcomb, T. A.; Heuer, W. B.; Heagy, M. D.; Thompson, J.; Musselman, R. L.; Jacobsen, C. S.; Hoffman, B. M.; Ibers, J. A. To be submitted for publication in *Inorg. Chem.*
(45) Heagy, M. D. Unpublished work.

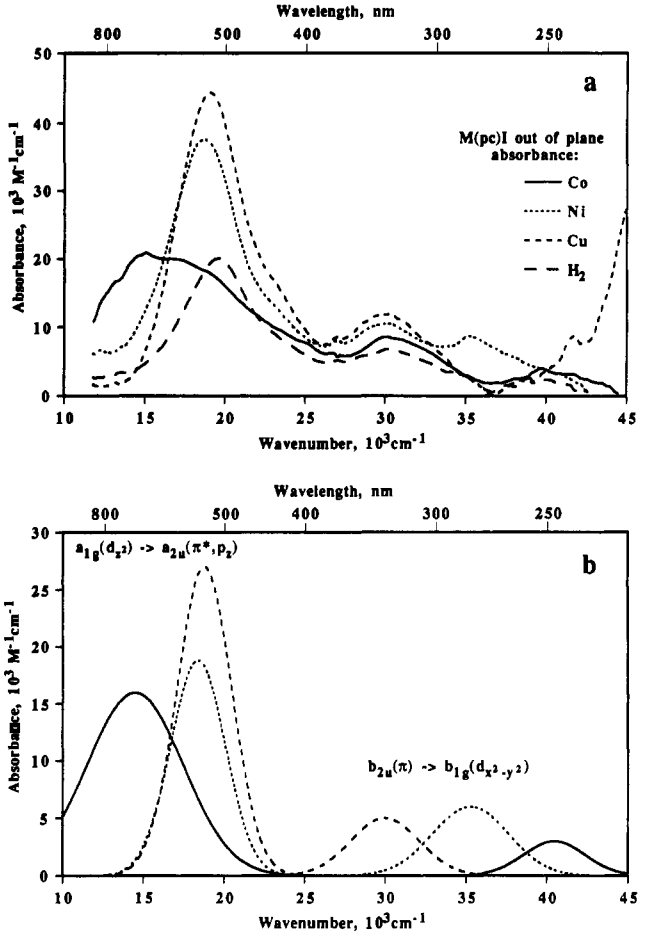


**Figure 5.** Out-of-plane absorbance spectra of M(pc)I's: (a) experimental spectra; (b) MLCT ($12a_{1g}(d_{z^2}) \rightarrow 6a_{2u}(\pi^*,p_z)$) and LMCT ($3b_{2u}(\pi) \rightarrow 11b_{1g}(d_{x^2-y^2})$) Gaussian peaks. Key: (—) Co(pc)I; (···) Ni(pc)I; (- - -) Cu(pc)I; (– – –) $H_2$(pc)I.

$11b_{1g}(d_{x^2-y^2})$ are shown for the three metallophthalocyanines in Figure 5b. In each case, the transition energies follow predictions from simple considerations of metal energy levels.

**In-Plane Transitions.** Transitions allowed when the electric vector is aligned parallel to the plane of the pc macrocycle are more numerous than those allowed out of plane. As in porphyrins also,[7] the principal features are prominent visible transitions at ~15 000 $cm^{-1}$ ("Q") and large ultraviolet transitions at ~30 000 $cm^{-1}$ ("B" or "Soret").

**(1) Theoretical Models.** The well-known four-orbital model of porphyrin rings[6,7,38] which has been used for decades as a basis for interpretation of porphyrinic spectra begins with two $a_{2u}$ and $a_{1u}$ HOMO's, which in porphyrins are assumed to be nearly degenerate, and an $e_g$ pair of LUMO's. The nearly identical energies of the $a_{1u}{}^1e_g{}^1$ and $a_{2u}{}^1e_g{}^1$ states allows sufficient configuration interaction (CI) so that one combination of excited states, the B state, is ~15 000 $cm^{-1}$ above the other, the Q state. Thus, the four-orbital model is energetically consistent with experiment. The CI in porphyrins results in the Q transition's being forbidden, which is consistent with Q typically being about $^1/_{10}$ the intensity of B in porphyrins. In phthalocyanines, on the other hand, the visible transitions are close to the same intensity as the Soret band in the ultraviolet. The explanation for this difference was found through extended Hückel calculations on porphyrins and phthalocyanines,[46] which showed a much greater energy difference between $a_{1u}$ and $a_{2u}$ in a typical phthalocyanine (Zn(pc)) than for the corresponding porphyrin (Zn(p)) or tetrabenzoporphyrin (Zn(tbp)). This essentially eliminates CI for the two excited states $a_{1u}{}^1e_g{}^1$ and $a_{2u}{}^1e_g{}^1$, which removes the forbiddenness of the lower energy transition, and thus the visible band is much larger in the pc's. The largest visible transition, still named Q, even though it is no longer a result of state mixing, was thus assigned by Gouterman[7] as pure $a_{1u} \rightarrow e_g$, and the ultraviolet transition, B, was assigned as pure $a_{2u} \rightarrow e_g$. It is interesting to note that the energies of Q and B are in the same regions for both p's and pc's, and thus the energy difference attributed to CI in the porphyrins is now a straight orbital energy difference in pc's according to this traditional interpretation.

Around the same time that Gouterman et al. were developing their models, a well-conceived semiempirical model was presented for Cu(p),[47] Cu(pc),[36] and $H_2$(pc).[35] This model differs significantly from Gouterman's model in that several electronic transitions are predicted for each of the several regions (Q, B, N, L, C) which Gouterman had proposed as being individual electronic transitions.[7] This work has recently been used in interpreting absorption and MCD spectra of Zn(pc).[8] A more recent calculation comparing Ni(tbp) (tbp = tetrabenzoporphyrin) with Ni(pc)[34] using a discrete variational X$\alpha$ (DVX$\alpha$) method has proven useful in comparing energies of MLCT and LMCT transitions in Co(pc)I and Ni(pc)I.[21] Very recently, Ellis et al.[37] using a density of states (DOS) variation of the DVX$\alpha$ method have calculated transitions in pc's that agree especially well with experiment. In our interpretation of the in-plane spectra for Cu(pc)I and $H_2$(pc)I, as well as a reexamination of our Co(pc)I and Ni(pc)I work, we will attempt to make assignments only so far as the calculations seem consistent. In many cases, especially in the higher energy UV region, specific assignment is still not feasible due to the multitude of transitions apparent.

**(2) Cu(pc)I, Visible Region.** Table I summarizes the experimental transition energies and the proposed orbital transition assignments for Co-, Ni-, Cu-, and $H_2$(pc)I and the theoretical calculated energies of transitions with oscillator strengths of 0.2 or greater for Co-, Ni-, and Cu(pc).[37] Calculations by Henriksson et al. for Cu(pc) and $H_2$(pc) are not included since specific assignments are not available.[35,36] Figure 4b shows the transformed in-plane spectrum for Cu(pc)I with deconvolution into Lorentzian (Q) and Gaussian (all others) curves. Peak Q at 15.2 × $10^3$ $cm^{-1}$ is the peak closest to the calculated energies of 13.1 × $10^3$ $cm^{-1}$ for the $2a_{1u}(\pi) \rightarrow 7e_g(\pi^*)$ ($E_u$) transition[37] and 18.4 × $10^3$ $cm^{-1}$ for an unspecified $E_u$ transition.[36] This peak has been assigned as $a_{1u} \rightarrow e_g$ by Gouterman et al.,[48] and it is thus consistent to assign peak Q as $2a_{1u}(\pi) \rightarrow 7e_g(\pi^*)$. Peak R at 18.0 × $10^3$ $cm^{-1}$ has had an uncertain history, having been proposed to be either a vibronic component of the Q band[49] or a splitting of Q due to a lowered site symmetry.[21,48,50] (This latter effect is to be distinguished from a lowered *molecular* symmetry as appears in $H_2$(pc), which is $D_{2h}$ rather than $D_{4h}$ as in M(pc's).) In $D_{4h}$ systems, up to three peaks in this region have been reported in room-temperature studies,[8,51] traditionally labeled as Q(0,0) (the peak labeled herein as Q), Q(1,0), and Q(2,0), since it was believed that the extra one or two peaks to the blue of Q were vibronic components of the electronic transition at Q. Low-temperature studies of both porphyrins and phthalocyanines[52-55] have shown numerous vibrational peaks to exist under the three envelopes in question demonstrating that the labels (0,0), (1,0), and (2,0) do not accurately represent the nature of these peaks. In addition, several experimental[51,56,57] and theoretical[36,37] studies have proposed that at least one additional electronic transition resides in the

(46) Schaffer, A. M.; Gouterman, M.; Davidson, E. R. *Theoret. Chim. Acta* **1973**, *30*, 9.
(47) Roos, B.; Sundbom, M. *J. Mol. Spectrosc.* **1970**, *36*, 8.
(48) Edwards, L.; Gouterman, M. *J. Mol. Spectrosc.* **1970**, *33*, 292.
(49) Marks, T. J.; Stojakovic, D. R. *J. Am. Chem. Soc.* **1978**, *100*, 1695.
(50) Day, P.; Scregg, G.; Williams, R. J. P. *J. Chem. Phys.* **1963**, *38*, 2778.
(51) VanCott, T.; Rose, J.; Misener, G. C.; Williamson, B.; Schrimpf, A.; Boyle, M.; Schatz, P. *J. Phys. Chem.* **1989**, *93*, 2999.
(52) Radziszewski, J. G.; Waluk, J.; Michl, J. *J. Mol. Spectrosc.* **1990**, *140*, 373.
(53) Fitch, P.; Haynam, C.; Levy, D. *J. Chem. Phys.* **1981**, *74*, 6612.
(54) Kooter, J. A.; Van Der Waals, J. H. *Mol. Phys.* **1979**, *37*, 1015.
(55) Huang, T.-H.; Rieckhoff, K. E.; Voigt, E. M. *J. Chem. Phys.* **1982**, *77*, 3424.
(56) Fitch, P. M.; Sharton, L.; Levy, D. H. *J. Chem. Phys.* **1979**, *70*, 2018.
(57) Metcalf, D. H.; VanCott, T. C.; Snyder, S. W.; Schatz, P. N.; Williamson, B. E. *J. Phys. Chem.* **1990**, *94*, 2828.

high-energy shadow of peak Q. In view of this, we have chosen not to use the Q(1,0) and Q(2,0) labels for peaks in this region since they are misleading. However we will use the traditional labels B, N, L, and V for segments of the UV region of the spectrum, with the caveat that we shall point out that multiple electronic transitions may lie under each of these latter regions. In view of the very different nature of the vibrational fine structure in regions $\sim 15.3 \times 10^3$ cm$^{-1}$ and $\sim 16.7 \times 10^3$ cm$^{-1}$ [56,57] and the similarity of these regions in both the vapor state[48] and solid state,[21] it appears that the proposal of lowered site symmetry as the origin of R is not correct. Peak R is most likely due to a combination of vibrational overtones from Q and an additional electronic transition. Henriksson et al.[36] have proposed that a $\pi \rightarrow \pi^*$ $E_u$ transition calculated to lie at $21.6 \times 10^3$ cm$^{-1}$ may be partly responsible for the intensity to the blue of Q. Ellis et al.[37] calculate that the $5a_{2u}(\pi) \rightarrow 7e_g(\pi^*)$ lies at $15.4 \times 10^3$ cm$^{-1}$ for Cu(pc), with an oscillator strength, $f$, of 1.25 compared with $f = 2.04$ for the Q transition. This excellent agreement in relative energy between peaks Q and R ($2.6 \times 10^3$ cm$^{-1}$) and the calculated values for $2a_{1u} \rightarrow 7e_g$ vs $5a_{2u} \rightarrow 7e_g$ ($2.3 \times 10^3$ cm$^{-1}$) and the qualitative agreement with relative intensities indicates that it is reasonable to assign peak R as primarily $5a_{2u}(\pi) \rightarrow 7e_g(\pi^*)$.

Another $a_{2u} \rightarrow e_g$ transition, $4a_{2u}(\pi) \rightarrow 7e_g(\pi^*)$, was calculated[37] to lie at $23.5 \times 10^3$ cm$^{-1}$ in Cu(pc) with $f = 0.20$. Two other transitions were calculated to have similar energies and intensities: $2b_{1u} \rightarrow 7e_g$ at $25.5 \times 10^3$ cm$^{-1}$ with $f = 0.36$ and the $6e_g(\pi) \rightarrow 3b_{1u}(\pi^*)$ at $23.6 \times 10^3$ cm$^{-1}$ with $f = 0.36$. The experimental peaks labeled as S and T may result from these three transitions. Largely because of good energy and intensity agreement in this region between calculation and experiment in the Ni(pc) and Co(pc) cases (vide infra), we are tentatively assigning peak S as $2b_{1u} \rightarrow 7e_g$ and T as $4a_{2u} \rightarrow 7e_g$ and $6e_g \rightarrow 3b_{1u}$. One of the latter transitions, of course, could easily reside elsewhere in the region above $25 \times 10^3$ cm$^{-1}$, since they are predicted to be weak transitions.

**(3) Cu(pc)I, Soret Region.** The large experimental in-plane-polarized intensity between 28 and $45 \times 10^3$ cm$^{-1}$ apparently arises from several intense transitions. The calculations by Ellis et al.[37] predict six transitions in this region with oscillator strengths of 0.20 or greater, as noted in Table I. The peaks visible atop this region of absorption in phthalocyanines have traditionally been labeled as B, N, and L.[42,48] Since there are many more than four transitions in this region, we will use these labels as referring to regions rather than specific transitions. In generating Gaussian deconvolution, we started with the four energies experimentally evident: the shoulder at $29.0 \times 10^3$ cm$^{-1}$, the large maximum at $31.0 \times 10^3$ cm$^{-1}$, and the two maxima at $35.0 \times 10^3$ and $37.5 \times 10^3$ cm$^{-1}$. The latter three peaks have been identified in numerous phthalocyanines as peaks B, N, and L, respectively, by Gouterman.[48] A fifth peak at $32.5 \times 10^3$ cm$^{-1}$ developed as a residual following subtraction of the other four. As will be seen in the Co-, Ni-, and $H_2$(pc)I spectra, there is consistently a strong, dominant peak close to $30 \times 10^3$ cm$^{-1}$. As shown in Table I, the $6e_g \rightarrow 4b_{2u}$ transition is predicted[37] to be uniformly intense and close to $32 \times 10^3$ cm$^{-1}$ in all cases. This peak is known as the Soret band but has been assigned by Gouterman[58] as $4a_{2u}(\pi) \rightarrow 6e_g(\pi)$. This is in fact the same transition as we assigned to peak R, since the orbitals are the highest occupied $a_{2u}$ and lowest unoccupied $e_g$ orbitals. Due to differences in orbital numbering related to valence electron counting, Ellis' $5a_{2u}$ and $7e_g$ orbitals are equivalent to Gouterman's $4a_{2u}$ and $6e_g$ orbitals, respectively. We have chosen not to characterize peak R as the Soret transition even though its orbital transitions agree with earlier assignments of the Soret band, since the nomenclature was attributed[6] primarily to the strong $30 \times 10^3$ cm$^{-1}$ peak rather than to a specific orbital transition. Calculations by Henriksson et al.[36] attribute four $x,y$-polarized $\pi \rightarrow \pi^*$ transitions to the B region: two strong transitions at $34.5 \times 10^3$ and $35.3 \times 10^3$ cm$^{-1}$ and two weak transitions at $34.4 \times 10^3$ and $36.6 \times 10^3$ cm$^{-1}$. Recent experimental work on Zn(pc)[51] has also suggested more than one transition in the B region. We are thus not the first to suggest transitions other than $a_{2u} \rightarrow e_g$ to the B region. Since the $5a_{2u} \rightarrow 7e_g$ has already been assigned to peak R, and the next higher energy $a_{2u} \rightarrow e_g$ transition, $4a_{2u} \rightarrow 7e_g$, is predicted to be weak ($f = 0.2$), it seems reasonable to now reassign the Soret or B band at $31.0 \times 10^3$ cm$^{-1}$ in Figure 4b as being largely due to the $6e_g \rightarrow 4b_{2u}$ transition.

Peak U in Cu(pc)I is a relatively strong transition to the red of band B. A strong transition is predicted slightly to the blue of B by Ellis's calculations[37] as shown in Table I, the $6e_g \rightarrow 6a_{2u}(\pi^*,p_z)$ transition. Ellis et al. did not include metal $p_z$ orbitals in these calculations, and thus we need to call upon some experimental results to consider the effect of not only individual atomic $p_z$'s but the effects due to overlapping $p_z$ orbitals in a stacking arrangement on the predicted energy for a $6e_g \rightarrow 6a_{2u}$ transition. The first expectation is that combination with a $p_z$ metal orbital would lower the $6a_{2u}$ level in the single molecule. Further suggestions of lowering come from a consideration of experimental results on the solid state vs an isolated solution or gaseous complex in analogous systems. In other square-planar transition-metal complexes with unsaturated ligands, i.e., $Pt(CN)_4^{2-}$,[27,59] $Pd(CN)_4^{2-}$,[26] $Ni(CN)_4^{2-}$,[60] and $Ni(dmg)_2$,[28] we and others have found that, as the metal complex planes stack closer together as a result of changes in cations, a peak assigned as $a_{1g}(d_{z^2}) \rightarrow a_{2u}(\pi^*,p_z)$ dramatically red shifts (by up to $19 \times 10^3$ cm$^{-1}$). The $x,y$-polarized $e_g(d_{xz,yz}) \rightarrow a_{2u}(\pi^*,p_z)$ transition nearby in energy in solution shows about 25% of the red shift of the $a_{1g} \rightarrow a_{2u}$ transition.[60] We attribute part of the red shift to a lowering of the $p_z$ orbital on the metal due to interaction along the metal chain. The same process appears likely in the M(pc)I case, where a lowering of $p_z$ due to an as yet undetermined mechanism (neither factor group splitting, exciton formation, nor band formation is alone sufficient to explain the mechanism) causes the $6a_{2u}$ orbital to be lower than in the single molecule case. Thus, we would expect the $6e_g(\pi) \rightarrow 6a_{2u}(\pi^*,p_z)$ transition to appear at a lower energy than calculated.[37] Peak U fits this description and is therefore tentatively assigned as this transition.

**(4) Cu(pc)I, High-UV Region.** The remainder of the UV absorptions, including bands N and L, also is expected to be due to several transitions. Henriksson et al.[36] predict four weak $\pi \rightarrow \pi^*$ transitions in the N band region, at $39.6 \times 10^3$, $39.7 \times 10^3$, $40.1 \times 10^3$, and $41.8 \times 10^3$ cm$^{-1}$ and several weak $\pi \rightarrow \pi^*$ transitions and one strong $\pi \rightarrow \pi^*$ transition in the L region. As a practical matter, though, it is difficult to assign calculated transitions to specific peaks when intensities are similar and energies close. Ellis et al.[37] have calculated that at least four moderate transitions, $5e_g(\pi,d_{xz,yz}) \rightarrow 3b_{1u}(\pi^*)$, $6e_g \rightarrow 3a_{1u}$, $3b_{2u} \rightarrow 8e_g$, and $2b_{1u} \rightarrow 8e_g$ fall between $32 \times 10^3$ and $40 \times 10^3$ cm$^{-1}$. Although the relative prominence of peak N suggests it is due to the $3b_{2u} \rightarrow 8e_g$ transition, calculated to have an oscillator strength of 0.95 (and this transition is also calculated to be the strongest one in this region for Co(pc) and Ni(pc)[37]), the similarity of energies and intensities for transitions in this region (see Table I) makes specific assignments difficult. We thus attribute peaks V, N, and L and the intensity just beyond $40 \times 10^3$ cm$^{-1}$ collectively to $3b_{2u} \rightarrow 8e_g$, $2a_{1u} \rightarrow 9e_g$, $2b_{1u} \rightarrow 8e_g$, and $5e_g \rightarrow 3a_{1u}$ transitions.

**(5) Co(pc)I and Ni(pc)I Revisitation.** Before interpreting the in-plane $H_2$(pc)I spectrum, it seems reasonable to reiterate and modify our earlier assignments of the Co(pc)I and Ni(pc)I in-plane spectra[21] in light of the above discussion. In both Co(pc)I and Ni(pc)I, whose in-plane spectra are shown in Figures 6 and 7, respectively, the assignment of the lowest energy in-plane transition, peak Q, as $a_{1u}(\pi) \rightarrow e_g(\pi^*)$ is confirmed as a $2a_{1u}(\pi) \rightarrow 7e_g(\pi^*)$ transition. The next higher energy peak at $\sim 17.7 \times 10^3$ cm$^{-1}$, R, needs reassignment as a $5a_{2u} \rightarrow 7e_g$ transition in both cases. The $(20\text{–}28) \times 10^3$ cm$^{-1}$ regions in both spectra show evidence for two small transitions, peak S at $24 \times 10^3$ and peak T at $26.5 \times 10^3$ cm$^{-1}$ with peak S of lower intensity than peak

(58) Gutterman, D. F.; Gray, H. B. *J. Am. Chem. Soc.* **1971**, *93*, 3364.
(59) Yersin, H.; Gliemann, G. *Ann. N.Y. Acad. Sci.* **1978**, *313*, 539.
(60) Musselman, R. L. To be submitted for publication in *Inorg. Chem.*

**Table I.** Experimental and Calculated Phthalocyanine Transitions

| | | Co(pc)I theoret[a] | | | Ni(pc)I theoret[a] | | | Cu(pc) theoret[a] | | | |
|---|---|---|---|---|---|---|---|---|---|---|---|
| transition label | orbital transitions[a] | energy, $10^3$ cm$^{-1}$ | oscillator strength, $f$ | Co(pc)I exptl energy, $10^3$ cm$^{-1}$ | energy, $10^3$ cm$^{-1}$ | oscillator strength, $f$ | Ni(pc)I exptl energy, $10^3$ cm$^{-1}$ | energy, $10^3$ cm$^{-1}$ | oscillator strength, $f$ | Cu(pc)I exptl energy, $10^3$ cm$^{-1}$ | $H_2$(pc)I exptl energy, $10^3$ cm$^{-1}$ |
| out-of-plane | $12a_{1g}(d_z2) \rightarrow 6a_{2u}(\pi^*,p_z)$ | | | A 14.5 | | | A 18.4 | | | A 18.8 | |
| | $I_3^-$: $^1\Sigma_g \rightarrow {}^1\Sigma_u^*$ | | | D 20.0 | | | D 20.0 | | | D 19.9 | D 19.6 |
| | $I_3^-$: solid-state trans | 17.2 | 3.2 | E 25.0 | 17.2 | 3.2 | E 24.5 | 17.2 | 3.2 | E 24.0 | E 24.1 |
| | $I_3^-$: spin–orbit comp of B | | | F 30.1 | | | F 30.0 | | | F 30.0 | F 30.0 |
| | $3b_{2u}(\pi) \rightarrow 11b_{1g}(d_{x^2-y^2})$ | | | G 40.5 | | | G 35.3 | | | G 30.0 | |
| | | | | | | | | | | H 34.0 | H 34.5 |
| | | | | | | | | | | | H′ 39.2 |
| in-plane | | | | | | | | | | | |
| Q | $2a_{1u}(\pi) \rightarrow 7e_g(\pi^*)$ | 12.6 | 1.67 | Q 15.7 | 12.1 | 1.59 | Q 15.8 | 13.1 | 2.04 | Q 15.2 | Q 15.1 |
| | $5a_{2u}(\pi) \rightarrow 7e_g(\pi^*)$ | 22.3 | 1.00 | R 19.0 | 22.0 | 0.93 | R 18.5 | 15.4 | 1.25 | R 18.0 | R 17.1 |
| | | | | | | | | | | | R′ 18.8 |
| | $2b_{1u}(\pi) \rightarrow 7e_g(\pi^*)$ | 21.8 | 0.36 | S 24.0 | 21.1 | 0.34 | S 24.0 | 25.5 | 0.36 | S 27.1 | S 25.0 |
| | $4a_{2u}(\pi) \rightarrow 7e_g(\pi^*)$ | 26.9 | 0.59 | T 26.5 | 28.9 | 0.64 | T 27.0 | 23.5 | 0.2 | T 24.9 | T 27.3 |
| | $6e_g(\pi) \rightarrow 3b_{1u}(\pi^*)$ | 30.5 | 0.24 | | 32.0 | 0.23 | | 23.6 | 0.36 | T′ 24.9 | |
| Soret[b] | $6e_g(\pi) \rightarrow 4b_{2u}(\pi^*)$ | 32.4 | 0.83 | B 31.4 | 31.8 | 0.75 | B 30.5 | 32.3 | 0.75 | B 31.0 | B 31.2 |
| | $6e_g(\pi,d_{xz,yz}) \rightarrow 6a_{2u}(\pi^*,p_z)$ | 36.1 | 0.37 | U 29.9 | 37.1 | 0.34 | | 35.8 | 0.73 | U 29.0 | |
| | $5e_g(\pi,d_{xz,yz}) \rightarrow 3b_{1u}$ | | | | | | | 32.4 | 0.26 | V 32.5 | |
| | $6e_g(\pi) \rightarrow 3a_{1u}(\pi^*)$ | | | | | | | 36.1 | 0.25 | L 37.8 | |
| | $3b_{2u}(\pi) \rightarrow 8e_g(\pi^*)$ | 41.4 | 0.74 | N 35.1 | 42.2 | 0.64 | V 34.5 | 34.5 | 0.95 | N 35.0 | N 35.2 |
| | $2a_{1u}(\pi) \rightarrow 9e_g(\pi^*)$ | 41.4 | 0.50 | V 37.3 | 41.7 | 0.55 | | | | | V 37.9 |
| | $2b_{1u}(\pi) \rightarrow 8e_g(\pi^*)$ | 41.1 | 0.45 | L 39.5 | 41.4 | 0.46 | N 36.8 | 43.9 | 0.36 | X >40.0 | L 39.9 |
| | $5e_g(\pi,d_{xz,yz}) \rightarrow 3a_{1u}(\pi^*)$ | 40.7 | 0.60 | W 42.0 | 40.9 | 0.51 | L 40.0 | | | | |

[a] Calculations from ref 37. [b] Principal contribution to the B, or Soret, band. See text for details.

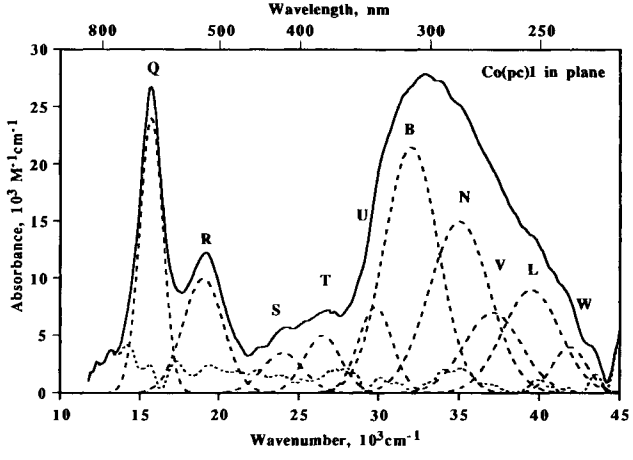


**Figure 6.** Absorbance from in-plane-polarized specular reflectance spectrum of Co(pc)I: (—) experimental; (---) Gaussian deconvolution; (···) residual baseline.

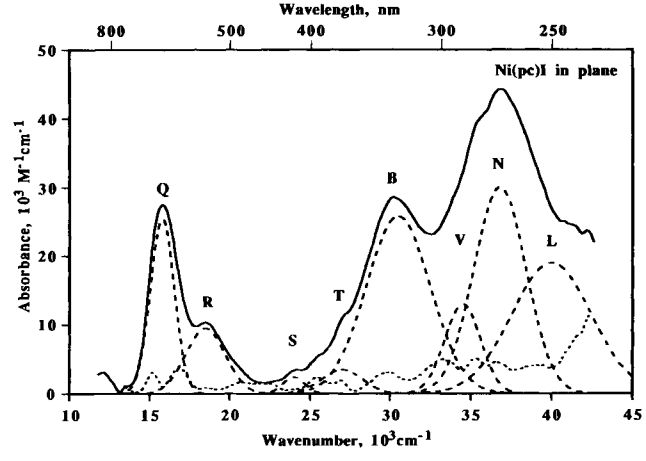


**Figure 7.** Absorbance from in-plane-polarized specular reflectance spectrum of Ni(pc)I: (—) experimental; (---) Gaussian deconvolution; (···) residual baseline.

T in both cases. This relationship of energies and intensities agrees with the calculations of Ellis et al.[37] for the $2b_{1u} \rightarrow 7e_g$ (at (21.5 ± 0.4) × $10^3$ $cm^{-1}$, $f \approx 0.35$) and $4a_{2u} \rightarrow 7e_g$ (at (27.9 ± 1.0) × $10^3$ $cm^{-1}$, $f \approx 0.61$) transitions, and thus it is reasonable to assign peaks S and T as $2b_{1u} \rightarrow 7e_g(\pi^*)$ and $4a_{2u}(\pi) \rightarrow 7e_g(\pi^*)$, respectively. These had been noted earlier[21] as undeterminable.

In the region of (28–45) × $10^3$ $cm^{-1}$ we earlier proposed[21] at least three transitions, the lowest energy transition being $a_{2u} \rightarrow e_g(\pi)$, which, as noted in the Cu(pc)I case, appears actually to be a small contribution to this region. The Ni(pc)I in-plane spectrum in Figure 7 shows good resolution of the Soret transition, peak B. In a more clear case than with Cu(pc)I, the $6e_g \rightarrow 4b_{2u}$ transition was calculated to be the most intense in the 30 × $10^3$ $cm^{-1}$ region and may thus be assigned to peak B. While the Co(pc)I spectrum (Figure 6) is not resolved, a reasonable deconvolution yields a prominent peak B at 31 × $10^3$ $cm^{-1}$, which we will also assign as $6e_g \rightarrow 4b_{2u}$, since Ellis's calculations for Co(pc) are very similar to those for Ni(pc). This leaves a hunt for peak U, tentatively assigned in Cu(pc)I as $6e_g(\pi) \rightarrow 6a_{2u}(\pi^*,p_z)$. In Co(pc)I, one sees a moderately weak peak showing as a slight shoulder at ~30 × $10^3$ $cm^{-1}$. The $6e_g \rightarrow 6a_{2u}$ transition in both Co(pc) and Ni(pc) was predicted to be less than half as intense as that in Cu(pc),[37] and peak U in Co(pc)I is consistent with that expectation. In Ni(pc)I, this transition may be hidden under peak B.

The remainder of the intensity, above peak B, is difficult to specify, since for both Ni(pc) and Co(pc) Ellis' calculations predicted four transitions of nearly equal energies (~41 × $10^3$ $cm^{-1}$) and intensities ($f$ = 0.45–0.74). In Co(pc), Gouterman[48] identified several numbered peaks attributed to the metals in this region. Ellis' calculations show, however, that $6e_g$ has only minor contribution from $d_{xz,yz}$ and that the principal metal contribution is at a much lower orbital energy, around the $5e_g$ orbital. Thus, most in-plane transitions in this region would have little or no metal character. We thus see no reason to differentiate characterizations for the Ni and Co cases and have chosen to continue the N and L terminology used by Gouterman for the other metallophthalocyanines. In the Co(pc)I spectrum it is reasonable to place several peaks under the high-energy side of the large (27–44) × $10^3$ $cm^{-1}$ absorption. Gouterman's spectra[48] show remarkable consistency with regard to the energies of peaks B, N, and L, being close to 30 × $10^3$, 35 × $10^3$, and 41 × $10^3$ $cm^{-1}$, respectively, for 10 metallophthalocyanines. We do find slight shoulders at ~36 × $10^3$ and ~40 × $10^3$ $cm^{-1}$ in the Co(pc)I spectrum, so we have fit peaks labeled N and L at these locations, which are also consistent with Ellis' calculations. Two additional peaks emerge, V and W, consistent with the calculations. In the Ni(pc)I spectrum, the shoulder at 35 × $10^3$ $cm^{-1}$, the peak at 36.5 × $10^3$ $cm^{-1}$, and the shoulder at 40 × $10^3$ $cm^{-1}$, the latter two being consistent with N and L locations, have been used to deconvolute this high-energy region. While a fourth transition is predicted[37] for this region, we are unable to justify additional peaks experimentally. No attempt is being made to assign any of the four transitions likely to contribute to this region, $3b_{2u} \rightarrow 8e_g$, $2a_{1u} \rightarrow 9e_g$, $2b_{1u} \rightarrow 8e_g$, and $5e_g \rightarrow 3a_{1u}$, to specific absorptions.

**(6) $H_2$(pc)I.** Since no equivalent calculations are available for $H_2$(pc), our interpretation of the in-plane $H_2$(pc)I spectrum will be based upon extrapolation of the Co, Ni, and Cu cases. The in-plane $H_2$(pc)I transitions (Figure 3b) appear to be similar to those for Cu(pc)I in spite of the expected $D_{2h}$ symmetry of $H_2$(pc)I, where two opposite pyrrole nitrogens contain the protons. An X-ray study[18] shows no unusual structure for the phthalocyanine; the tetragonal crystal structure reflects the $D_{4h}$ molecular symmetry. It appears that the partial oxidation which allows straight stacking of macrocycles and the crystalline environment have minimized structural and electronic effects from the two hydrogens, unlike $\alpha, \beta, \gamma, \delta$-tetraphenylporphine, which crystallizes in a triclinic form[61] and whose polarized in-plane spectra show distinct splitting of the $x$- and $y$-allowed ring transitions.[41] On the basis of the structure, we would not expect to see significant splitting of peaks in $H_2$(pc)I, and we will assign transitions assuming a $D_{4h}$ point group. Peak Q at 15.1 × $10^3$ $cm^{-1}$ corresponds to the $2a_{1u}(\pi) \rightarrow 7e_g(\pi^*)$ Q transition, and peak R at 17.1 × $10^3$ $cm^{-1}$ corresponds to the $5a_{2u}(\pi) \rightarrow 7e_g(\pi^*)$ transition. Peak R′ is only slightly above the noise level but if real may be a vibronic component of R. We are resisting the temptation to attribute it to $D_{2h}$ splitting, which, if present, would cause the $D_{4h}$ $2a_{1u}(\pi) \rightarrow 7e_g(\pi^*)$ transition to become $a_u \rightarrow b_{2g}$ (allowed $y$) and $a_u \rightarrow b_{3g}$ (allowed $x$) and the $5a_{2u}(\pi) \rightarrow 7e_g(\pi^*)$ transition to become $b_{1u} \rightarrow b_{2g}$ (allowed $x$) and $b_{1u} \rightarrow b_{3g}$ (allowed $y$). Since, in both cases, the split transitions are allowed and the overlap is equivalent, one would expect equal intensities for each pair. In the case of R and R′, the great difference in intensities argues against these being a $D_{2h}$ symmetry split pair. The same argument also holds for Q and R. Peaks S and T are also only suggested by the undulation in the experimental curve, but intensity is needed in that region consistent with their energies and band shape. As in the M(pc)I's, we will tentatively assign S and T as $2b_{1u} \rightarrow 7e_g$ and $4a_{2u} \rightarrow 7e_g$, respectively.

The large absorbance around (30–35) × $10^3$ $cm^{-1}$ is clearly the product of at least two transitions. We will assign peak B, as with the M(pc)I's, as $6e_g \rightarrow 4b_{2u}$. Peak N appears at first glance to be a good candidate for a symmetry-split equivalent transition to peak B. In $\alpha, \beta, \gamma, \delta$-tetraphenylporphine, however, where deviation from $D_{4h}$ symmetry and planarity (pyrrole N's up to 0.15 Å out of the plane) is significant,[61] the splitting of the Soret transition was ~2 × $10^3$ $cm^{-1}$.[41] In the case at hand, the energy difference between peaks B and N is greater than 5 × $10^3$ $cm^{-1}$. It does not seem reasonable to expect that this difference is due to symmetry splitting given the structure of $H_2$(pc) in $H_2$(pc)I.[18] We thus attribute peak N to one or more of the transitions $3b_{2u} \rightarrow 8e_g$, $2a_{1u} \rightarrow 9e_g$, $2b_{1u} \rightarrow 8e_g$, and $5e_g \rightarrow 3a_{1u}$. The latter is the least likely, since $5e_g$ contains a significant $d_{xz,yz}$ contribution in M(pc)I.[37]

**Conclusions.** The presence of the $a_{1g}(d_{z^2}) \rightarrow a_{2u}(p_z,\pi^*)$ transition characteristic of stacked square-planar transition-metal complexes has been confirmed in Co(pc)I and Ni(pc)I and found in Cu(pc)I. A second out-of-plane-polarized metal-related transition, $b_{2u}(\pi) \rightarrow a_{1g}(d_{x^2-y^2})$, has been found in Cu(pc)I in addition to Co- and Ni(pc)I, as reported earlier. Some in-plane transitions have been confirmed or reassigned as a result of recent calculations on Co(pc), Ni(pc), and Cu(pc): the low-energy Q band remains as a $2a_{1u}(\pi) \rightarrow 7e_g(\pi^*)$ transition, but the neighboring higher energy transition has been assigned primarily as a $5a_{2u}(\pi) \rightarrow 3e_g(\pi^*)$ transition, the lowest energy $a_{2u} \rightarrow e_g$ transition, rather than as a vibration or symmetry-split component of the Q band as has previously been suggested. Finally, the large intensity around 30 × $10^3$ $cm^{-1}$ characteristic of porphyrin systems, the Soret band, has been identified as primarily the $6e_g \rightarrow 4b_{2u}$ transition rather than an $a_{2u} \rightarrow e_g$ transition.

**Acknowledgment.** This work was supported by the donors of the Petroleum Research Fund, administered by the American Chemical Society (R.L.M.), by the National Science Foundation, through the Inorganic, Bioinorganic, and Organometallic Chemistry Program, Grant No. CHE-8911215 (R.L.M.), and the Solid State Chemistry Program, Grant No. DMR-8818599 (B.M.H.), by the Northwestern University Materials Research Center, Grant No. DMR-8821571 (B.M.H.), and by The Camille and Henry Dreyfus Foundation (New Grant Program in Chemistry for Liberal Arts Colleges to R.L.M.). Also acknowledged is Franklin & Marshall College for summer Hackman Fellowships to D.E.R. and M.D.H.

**Registry No.** Cu(pc)I, 95179-25-2; $H_2$(pc)I, 138059-68-4.

(61) Silvers, S.; Tulinsky, A. *J. Am. Chem. Soc.* **1964**, *86*, 927.